RESONANT TUNNELING BASED DEVICES

WITH MEMORY APPLICATIONS

By

DARRYL GENE WALKER

Bachelor of Science

in Electrical Engineering

Oklahoma State University

Stillwater, Oklahoma

1987

Submitted to the Faculty of the
Graduate College of
Oklahoma State University
in partial fulfillment of
the requirements for
the Degree of
MASTER OF SCIENCE
July, 1990

RESONANT TUNNELING BASED DEVICES

WITH MEMORY APPLICATIONS

Thesis Approved:

Thesis Advisor

Dean of the Graduate College

ACKNOWLEDGMENTS

I wish to express sincere appreciation to Dr. Chriswell Hutchens for his guidance and extreme patience throughout my graduate program. Thanks to Dr. Louis Johnson, and Dr. J. J. Lee for serving on my graduate committee.

To the Department of Electrical and Computer Engineering for supplying me with financial assistance to enable me to complete my eduacational goals.

To my parents Bricey and Birdie Walker, encouraged and instilled the desire in me to not only make, but also achieve my goals. Thanks to my brothers J. D. and Bill Walker and my sister Jacque Gore for making many long distance calls to extend their encouragement. Many thanks to Ralph Friend and Dr. Hans Bilger for providing friendship and advice whenever I needed it. I extend a sincere thank you to all of these people.

TABLE OF CONTENTS

LIST OF FIGURES

LIST OF TABLES

CHAPTER 1

INTRODUCTION

As integrated circuit technology approaches its theoretical limits in Bipolar Junction and MOS device density, the ability to achieve greater circuit density can only be obtained by the developement of new electronic devices. The limits of present Bipolar Junction and MOS devices are due to the domination of quantum mechanical effects as the device dimensions become smaller thus preventing the device from operating in the manner for which it was designed. It is only natural that a device that operates on the basis of quantum effects would be the choice for denser circuitry.

A quantum mechanical effect that can be used to make devices of interest is electron tunneling of which resonant tunneling is a special phenomena that exists in certain structures in which tunneling exists. Resonant tunneling is of special interest due to a region of negative differential resistance (NDR) in the current-voltage characteristics which will be shown in Chap. 2. This NDR makes a resonant tunneling device useful in a number of applications including: high frequency oscillators, multi leveled logic, analog to digital converters, infrared laser amplifiers, infrared optical detectors, and memory cells.

In chapter II the physics of a double barrier resonant tunneling diode (RTD) is dicussed. The transmission coefficient is derived and

the current-voltage characteristics of a double barrier RTD are discussed. Some design considerations for the RTD along with the material used to build these devices are discussed.

In chapter III resonant tunneling devices are reviewed. Switching limits and frequency limits of resonant tunneling diodes are also discussed.

In chapter IV a SPICE model for a resonant tunneling diode is presented and a new resonant tunneling diode memory cell is presented and analyzed.

Finally in chapter V conclusions are drawn about the memory structure presented and suggestions for further research are made.

CHAPTER II

THEORY OF RESONANT TUNNELING

Classical mechanics states that if a particle is traveling toward a potential barrier as in Fig. 2.1 with energy less than the potential energy of the barrier then the particle would be reflected at the barrier. It could not pass into the barrier (the classically forbidden region) and could only cross over the barrier if it had energy greater than or equal to the potential energy of the barrier.

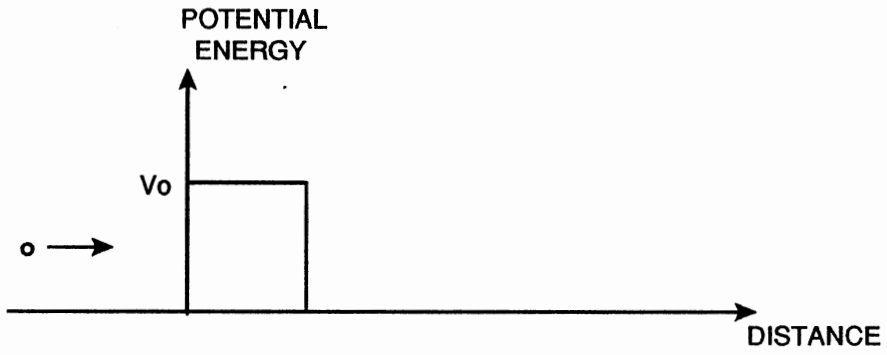

Figure 2.1 Particle traveling toward a potential barrier

With the developement of quantum mechanics, classical mechanics was shown to have inherent limitations when dealing with atomic

dimensions. One of these limitations was the possibility of a particle tunneling through a barrier as in Fig.2.1 (the equivalent of a person walking through a brick wall). This tunneling phenomena is the foundation of the topic of this thesis which investigates the work done in creating electronic devices based on resonant tunneling. This thesis developes a SPICE model for resonant tunneling and proposes a possibly useful
memory device based on resonant tunneling diodes.

Concepts of Tunneling

To understand the basic principle of tunneling consider a charge carrier (an electron) with effective mass m^* with energy E and wave vector k. The particle is incident on a step potential

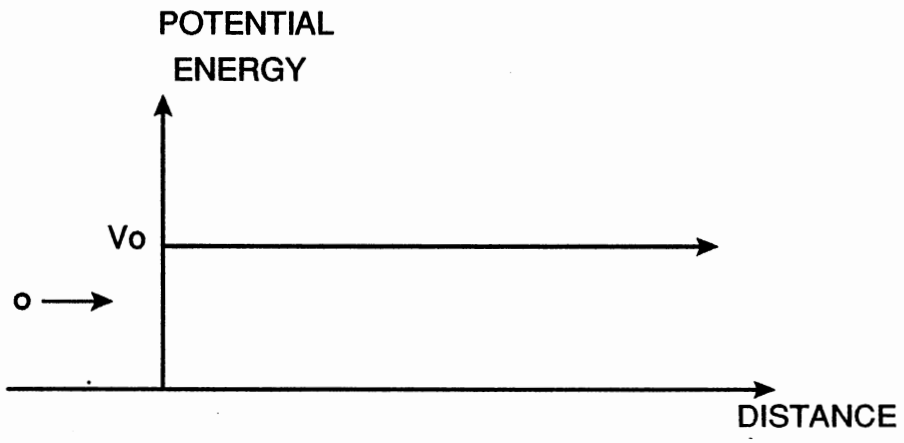

Figure 2.2. Particle traveling towards a step potential

(figure 2.2) $V(x)=0$ when $x<0$ and $V(x)= Vo$ when $x>0$.

The time independent Schrodinger equation can be written in one dimension as

$$-\frac{\hbar^2}{2m^*}\frac{\partial^2\Psi}{\partial x^2} + V(x)\Psi = E\Psi \qquad (2.1)$$

where Ψ is the wavefunction associated with the electron; $\hbar$ is plancks constant divided by 2π, $V(x)$ is the potential energy of the media, E is the energy of the electron corresponding to the wavefunction Ψ.

Equation (2.1) has the solution of the form

$$\Psi_1 = Ae^{jkx} + Be^{-jkx} \qquad (2.2)$$

where $$k = (2m^*E/h^2)^{1/2} \qquad (2.3)$$

Ψ consists of both an incident and reflected component.

$$\Psi_{inc} = Ae^{jkx} \qquad (2.4)$$

$$\Psi_{ref} = Be^{-jkx} \qquad (2.5)$$

In the region where $x>0$ the wavefunction can be written as

$$\Psi_2 = Ce^{-\alpha x} \qquad (2.6)$$

$$\text{where} \quad \alpha = \sqrt{\frac{2m^*(Vo-E)}{\hbar^2}} \tag{2.7}$$

There is no reflected wave in this region because of the continous potential energy of the media to the right of x=0.

From the fact that the wavefunction and its derivative must be continuous, $\Psi(0^-)=\Psi(0^+)$ and $\Psi'(0^-)=\Psi'(0^+)$. This allows the constant C in eq(2.6) to be solved in terms of A in eq(2.2).

The particle density inside the step potential is

$$\Psi^*_2\Psi_2 = 4\Psi^*_{inc}\Psi_{inc}\frac{e^{-2\alpha x}}{1+\frac{\alpha^2}{k^2}} \tag{2.8}$$

It can be seen that the particle density decays exponentially in the forbidden region with a decay length

$$l = \frac{1}{2\alpha} = \frac{\hbar}{2(2m^*(Vo-E))^{1/2}} \tag{2.9}$$

If the potential energy $Vo=\infty$ the particle density immediately falls off to zero and as $E\rightarrow Vo$ the particle density falls off very gradually with respect to x.

Since the wave function exists in the classically forbidden region, by making the step potential into a potential barrier with a small width (figure 2.1) the particle has a finite probability of tunneling through this classically forbidden region to the other side of the barrier.

The transmission coefficient (which is the probability that a particle is transmitted through the barrier) of such a barrier is found to be

$$T = \frac{1}{1 + \frac{1}{4}\left[\frac{k}{\alpha} + \frac{\alpha}{k}\right]^2 \sinh^2(\alpha L)} \qquad (2.10)$$

where k and α are as in equations (2.3) and (2.7).

Resonant Tunneling

In the case of two potential barriers separated by a quantum well as shown in fig. 2.3, the tunneling probability depends on the transmission coefficient of the individual barriers as well as the quasieigen states exsisting in the quantum well. The

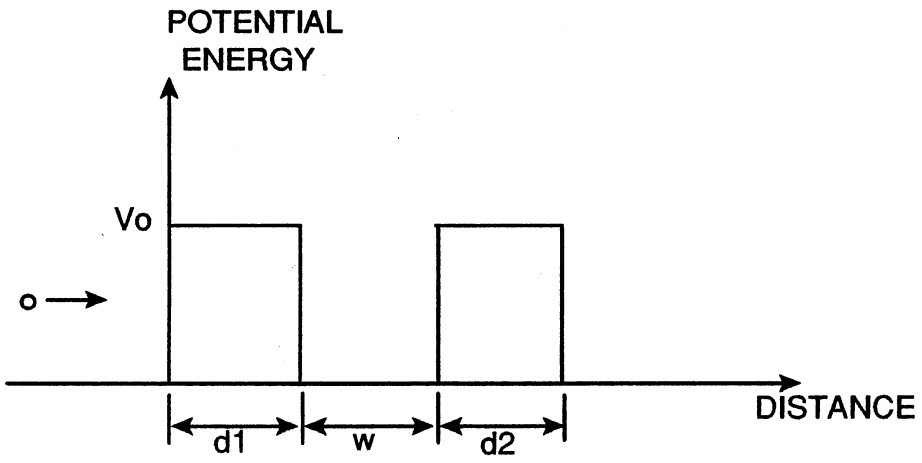

Figure 2.3. Two potential barriers separated by a quantum well

quasieigen states are located at energy levels that are capable of trapping an electron inside the well.

The quantum well is an energy filter. Since there are discrete occupiable energy states in the well, electrons with wave vectors that correspond to these levels can tunnel through the first barrier. These energy levels can be viewed by looking at the infinite potential well in figure 2.4.

If an electron is such that its energy matches one of the available eigenstates in the quantum well then the electron can be trapped in the quantum well. The wavefunction will bounce back and forth inside the well with small portions leaking out through each barrier until it reaches a resonance which is when the wavefunction leaking out of the well cancels the reflected wavefunction and enhances the transmitted (this is an effect equivalent to a Fabry Perot resonator).

This resonance greatly enhances the transmission coefficient of the structure, thus electrons will have a much higher probability of passing through the double barrier configuration at the resonance energy level than any other energy level.

The double barrier configuration is known as a resonant tunneling diode. These devices are created by growing thin layers of semiconductors with differing band gaps together as shown in fig. 2.5 along with their conduction and valence band energy profile.

These heterojunctions can be manufactured with layers down to an atomic thickness. Of course the compounds used must have very similar lattice structures or the lattice mismatches would cause defects in

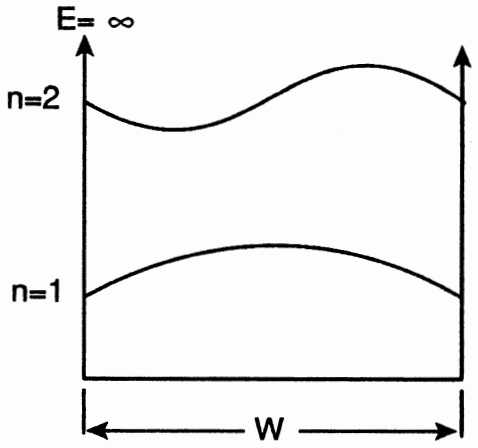

$$E = \frac{h^2 n^2}{8 m^* W^2}$$

Figure 2.4 Discrete energy states for an infinite potential well

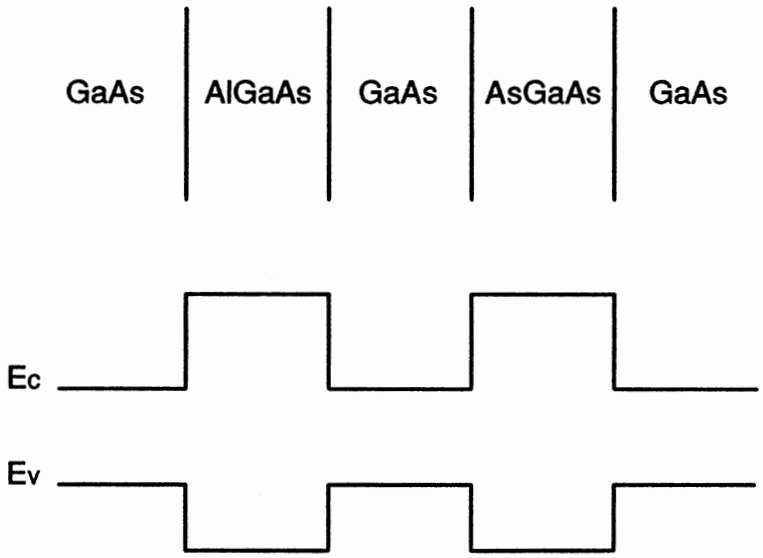

Figure 2.5 GaAs/AlGaAs resonant tunneling diode structure with with conduction and valence band diagrams

the device. Almost all of the work done in resonant tunneling has used III-V and II-VI compound semiconductors with the majority using GaAs-AlGaAs.

Resonant tunneling consists of two types of tunneling. Coherent resonant tunneling and incoherent resonant tunneling, which are clasified acording to the phase coherence of the electron's wavefunction after entering the double barrier structure.

Coherent Tunneling

As with any semiconductor device the electrons may suffer through elastic and inelastic scattering due to collisions with impurities and electron-electron scattering etc.

In the case that inelastic scattering is not present, phase coherence is not lost by the carriers the tunneling is said to be coherent resonant tunneling. Coherent resonant tunneling current through the double barrier structure is related to the transmission amplitude from region 1 to region 5 obtaining

$$t_{15} = t_{13}[1 + r_{35}r_{31} + (r_{35}r_{31})^2 \ldots\ldots]t_{35} \qquad (2.11)$$

t_{ab} is the transmission amplitude from region a to region b and r_{ab} is the reflection profile from region a to region b. The (N+1)th term expresses the probability amplitude of passing through the structure after bouncing back and forth inside the quantum well N times. Since the round trip deBroglie wavelength of the electron must be an

integral multiple of 2π, the wavefunction inside the well builds up to a resonance. The above equation is the binomial expansion of

$$t_{15} = \frac{t_{13}t_{35}}{1 - r_{35}r_{31}} \tag{2.12}$$

This equation is valid if and only if the energy of the carrier matches an available eigenstate in the quantum well.

To find the tunneling probability at resonance ($R_{ij} = |r_{ij}|^2$, $T_{ij} = v_j|t_{ij}|^2/v_i$, where v_i is the velocity in region i) assuming $v_1=v_2=v_3=v_4=v_5$ obtaining

$$T_{15}^{res} = \frac{T_{13}T_{35}}{\left[1 - \sqrt{R_{35}R_{31}}\right]^2} \approx \frac{4T_{13}T_{35}}{(T_{13} + T_{35})^2} \tag{2.13}$$

(Note $T_{15}^{res} = 1$ if $T_{13}=T_{35}$ and $T_{15}^{res} < 1$ if $T_{13} \neq T_{35}$)

There is a finite build up time τ_r which is associated with the time for the wavefunction to build up to a resonance inside the quantum well. A wave packet will bounce back and forth in the well a number of times to build up resonance. The time taken for one round trip in the well is 2d/v. (where d is the width of the well and v is the velocity of the wave packet inside the well). The transmision coefficent after N such round trips is obtained by summing the N+1 first terms of equation (2.11) obtaining

$$T_{15}(N) = T_{15}^{res}\left[1 - \left[\sqrt{R_{15}R_{31}}\right]^{N+1}\right]$$

$$\approx T_{15}^{res}\frac{N+1}{2}(T_{13} + T_{35}) \tag{2.14}$$

The resonance is fully developed when

$$\frac{N+1}{2}(T_{13} + T_{35}) \approx 1 \tag{2.15}$$

$$N \approx \frac{2}{T_{13} + T_{35}} \tag{2.16}$$

because T_{13} and T_{35} are very small.

The build up time τ_r is approximately

$$\tau_r = \frac{2dN}{v} = \frac{4d}{v(T_{13} + T_{35})} \tag{2.17}$$

The transmission coefficient for coherent tunneling can be written in terms of the full width at half maximum of the transmission resonant peak[74] and is

$$T_{coh} = T_{res}\frac{\frac{1}{2}\Gamma_e^2}{(E - E_r)^2 + \frac{1}{2}\Gamma_e^2} \tag{2.18}$$

which has a lorentzian energy dependence. Where Γ_e is the full width at half maximum (FWHM) of the transmission peak at the resonant energy. E_r is the resonant energy and E is the energy of the electron.

The FWHM of transmision coefficient at the resonant energy is related to the resonant buildup time by the Heisenburg uncertainty principle[13] giving

$$\Gamma_e = \frac{2\hbar}{\tau_r} \tag{2.19}$$

Substituting eq(2.17) into eq(2.19) gives

$$\Gamma_e = \frac{\hbar v (T_{13} + T_{35})}{2d} \tag{2.20}$$

It can now be seen that there is a trade off in choosing the width of a barrier since Γ_e and τ_r are related to the barrier widths. The wider the barrier the smaller is the transmission coefficient T_{ab} and the thinner the barrier the larger is T_{ab}. If $T_{13} + T_{35}$ is large then Γ_e is large, thus there is a broadening of the transmission peak at resonance. If $T_{13} + T_{35}$ is small the τ_r is large, which seriously inhibits the switching
time of a resonant tunneling device.

Calculation of Coherent RTD Current

The transfer matrix technique[68] can be used to calculate the transmission coefficient of a forward bias RTD. This technique requires the knowledge of four different types of matrices. As can be seen in figure 2.6 there are four cases of transmission. They are 1) transmission in classically allowed regions (d→e), 2) transmission in classically forbidden regions (b→c, f→g), 3) transmission accross a discontinuity from a classically allowed to a classically forbidden region (a→b, e→f) and 4) transmission accross a discontinuity from a classically forbidden to a classically allowed region (c→d, g→h). These matrices are called M_a, M_b, M_{in}, and M_{out} respectively. Using k and α as defined in eqns (2.3) and (2.7), the matrices are as follows.

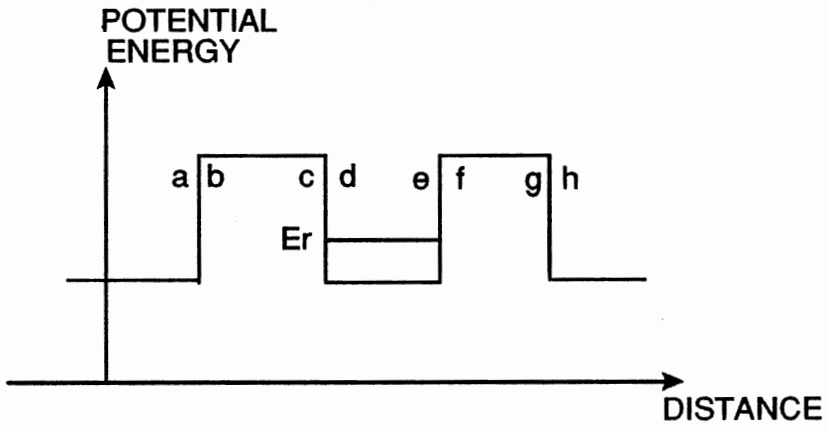

Figure 2.6 Illustration of regions for use of transfer matrix method of calculating the transmission coefficient of a resonant tunneling diode

$$M_a = \begin{bmatrix} e^{-ikd} & 0 \\ 0 & e^{ikd} \end{bmatrix} \tag{2.21}$$

$$M_b = \begin{bmatrix} e^{-\alpha d} & 0 \\ 0 & e^{\alpha d} \end{bmatrix} \tag{2.22}$$

$$M_{in} = \frac{1}{2} \begin{bmatrix} 1 - i\frac{\alpha}{k} & 1 + i\frac{\alpha}{k} \\ 1 + i\frac{\alpha}{k} & 1 - i\frac{\alpha}{k} \end{bmatrix} \tag{2.23}$$

$$M_{out} = \frac{1}{2} \begin{bmatrix} 1 + i\frac{k}{\alpha} & 1 - i\frac{k}{\alpha} \\ 1 + i\frac{k}{\alpha} & 1 + i\frac{k}{\alpha} \end{bmatrix} \tag{2.24}$$

When a potential difference is applied across the RTD structure the conduction band diagram appears as in figure 2.8. The potential drop in each region is dependent upon both the dielectric constant in that region and the region's width.

In the case of an applied potential difference across the RTD

$$(M_a)_{1,1} = \exp(-i\int k(x)\,dx$$

$$(M_a)_{2,2} = \exp(i\int k(x)\,dx \tag{2.25}$$

and

$$(M_b)_{1,1} = \exp(-\int\alpha(x)\,dx$$
$$(Mb)_{2,2} = \exp(\int\alpha(x)\,dx \tag{2.26}$$

where

$$\alpha 1(x) = \frac{1}{\hbar}\sqrt{2m^*(Vo - Ef - Fb(V)\cdot x)} \tag{2.27}$$

$$\alpha 2(x) = \frac{1}{\hbar}\sqrt{2m^*(Vo+w\cdot(Fb(V)-Fw(V))-Ef-Fb(V)\cdot x)} \tag{2.28}$$

$$k(x) = \frac{1}{\hbar}\sqrt{2m^*(Ef-(Fw(V)-Fb(V))\cdot d_1+Fw(V)\cdot x)} \tag{2.29}$$

$$Fb(V) = \frac{V}{d_1 + d_2 + w\cdot\frac{\varepsilon_b}{\varepsilon_w}} \tag{2.30}$$

$$Fw(V) = \frac{\varepsilon_b}{\varepsilon_w}\cdot Fb(V) \tag{2.31}$$

Where Ef is the Fermi level, Vo is the barrier potential, w is the well widty, d_1 and d_2 are the first and second barrier widths respectively, ε_b is the barrier dielectric constant and ε_w is the well dielectric constant.

The total transfer matrix is then found to be

$$M_{ah} = M_{ab}M_{bc}M_{cd}M_{de}M_{ef}M_{fg}M_{gh} \tag{2.32}$$

and the transmission coefficient of the RTD is

$$T_{ah} = \frac{1}{|M_{ah(1,1)}|^2} \tag{2.33}$$

The emitter of the resonant tunneling diode should be degeneratively doped to provide a supply of charge carriers. The collector region should be doped to minimize the ohmic resistance of the semiconductor, but not doped so heavily that there are too many electron states filled in the collector.(every state in the collector that is filled with an electron reduces the probability of tunneling from the emitter. The meeting of these criteria results in a coherent tunneling current density of[77]

$$J = \frac{qm^*kT}{2\pi^2\hbar^3} T \ln\left|\frac{1 + \exp[(Ef-E)/kT]}{1 + \exp[(Ef-E-V)/kT]}\right| dE \tag{2.34}$$

From eq (2.13) it is seen that the transmission peak is dependent upon the ratio of the transmission coefficient of each barrier at the resonant energy. It can be seen from fig. 2.7 that the electron is incident on the first barrier at a much lower energy relative to the potential of the barrier when a voltage is applied than the incident position of the second barrier assuming the electron doesn't descend or ascend energy levels in the quantum well. Thus the first barrier

has a much lower transmission coefficient than the second barrier (provided the barriers have the same dimensions). To optimize the double barrier transmission coefficient it is necessary to have the ratio $T_l/T_r = 1$ therefore the right barrier needs to be much thicker than the left barrier. This affect can be viewed from table I.

Incoherent Resonant Tunneling

If the scattering time of the electron is less than the build up time τ_r at the resonant energy, then the large current density in the well is never built up. This is due to inelastic scattering of the

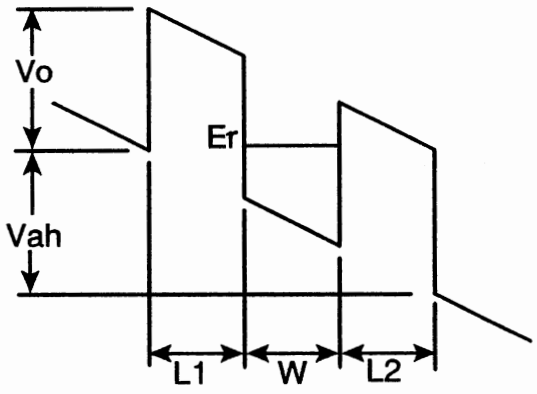

Figure 2.7 A forward biased resonant tunneling diode.

electrons in the barrier and well, thus causing phase cohenerece of the wavefunction to be lost. The scattering causes a decrease in the transmission peak at resonance and an increase in the transmission coefficient at off resonance energies.

TABLE I

PEAK TRANSMISSION OF A DOUBLE BARRIER RESONANT TUNNELING DIODES (AlGaAs/GaAs) FOR DIFFERENT EXIT BARRIER THICKNESS (L2)

L1 (Å)	W (Å)	L2 (Å)	Peak Transmission
50	50	50	0.45
50	50	60	0.97
50	50	70	0.72
50	50	80	0.21

Negative Differential Resistance and Peak to Valley Ratio

The desirable characteristic of a RTD is the negative differential resistance region just past the current peak as seen in figure 2.8 (the term negative differential resistance just implies $dI/dV < 0$). This quality gives rise to the applications specified in chapter 1. For most applications it is also desirable to have a large ratio between Ip and Iv as defined in figure 2.8 (current peak to valley ratio (PVR)). For example when using a RTD to build a high frequency oscillator the PVR determines the voltage swing of the

oscillator.

Since incohenrent tunneling causes an increase in transmission at off resonant energies, the PVR will degenerate when incoherent tunneling dominates. For optimal performance in most cases it is advantageous to have the major current component to mainly come from coherent tunneling effects.

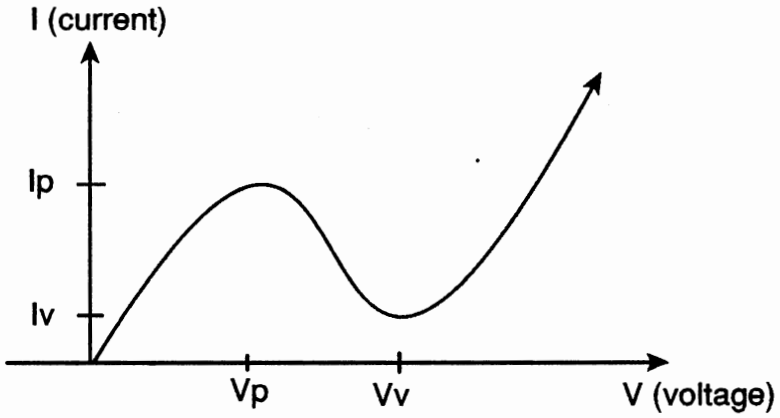

Figure 2.8 Current-voltage curve for a vevice with a negative differential resistance

Conclusion

The thicker the barriers the longer is the coherent tunneling buildup time. The thinner the barriers the greater the FWHM of the

transmission coefficient at the resonant peak, thus the smaller the peak to valley current ratio. These are the main concepts that have been discussed in this chapter and should be considered when designing a resonant tunneling diode.

CHAPTER III

RESONANT TUNNELING DEVICES

Introduction

Heterojunction superlattices and their electron transport properties were first investigated in 1970.[10] It was shown that if the superlattice has a period shorter than the mean free path of the electron then there would be a negative differential resistance region in the direction of the superlattice.

In 1973 the transport properties in a finite superlattice were calculated from a tunneling point of view and the I-V characteristics were computed for a few experimental cases including the double barrier case.[19]

This research led to the first construction of a double barrier resonant tunneling diode. This device was made by sandwiching a thin film of GaAs between two AlGaAs barriers.[7] The structures were fabricated using molecular beam epitaxy. The current and conductance characteristics of this device can be seen in Figure 3.1. The very small peak to valley ratio shows that the dominant tunneling current was due to incoherent tunneling. This was due to imperfections in the barriers and quantum well which greatly increase inelastic collisions by the charge carriers.

Circuit Model for a Resonant Tunneling Diode

A resonant tunneling diode has a equivalent circuit described in

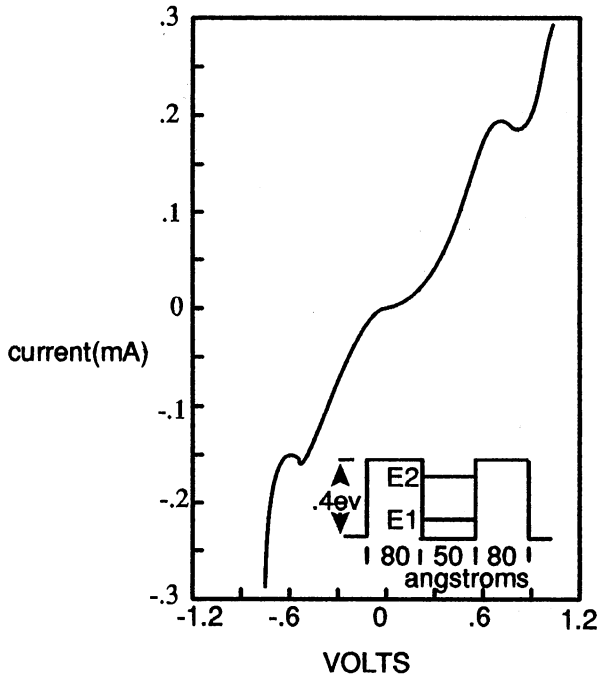

Figure 3.1 Current-voltage characteristics for resonant tunneling diode in the inset

figure 3.2. R_c and R_e are the bulk resistances of the collector and emitter regions respectively. C_q is the quantum capacitor due to the charge storage on both sides of the barrier regions. The variable resistance R_T has a region of negative differential resistance in its

characteristics. Due to the differences in doping R_c is usually at least an order of magnitude larger than R_e, thus R_e can usually be ignored

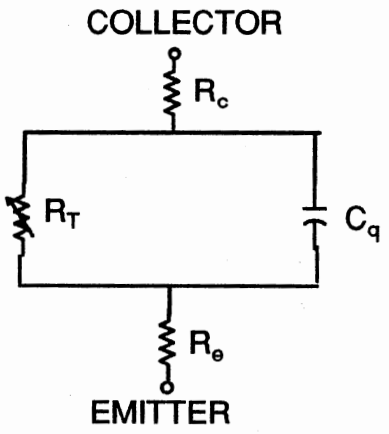

Figure 3.2 Equivalent circuit for a resonant tunneling diode

Osclillation Frequency Limit

A device with negative differential resistance characteristics can be used to make an oscillator.[11] The limit to the frequency of oscillation is dependent upon the magnitude of the negative differential resistance. The greater the negative slope in the I-V curves (i.e. the smaller the negative differential resistance), the greater will be the frequency limit of oscillation.

The oscillation frequency limit when using a resonant tunneling

diode to create the oscillator is not only limited by the negative differential resistance but also by R_c and C_q. The maximum frequency of oscillation achievable using a resonant tunneling diode is[8]

$$f_{max} = \frac{1}{2\pi C_q \sqrt{R_c R_N}} \tag{3.1}$$

Where R_N is the magnitude of the negative differential resistance. Table II shows some oscillation frequencies achieved with resonant tunneling diodes.

TABLE II

MAXIMUM FREQUENCY OF OSCILLATION OBSERVED IN RESONANT TUNNELING DIODES

f_{max}	Reference
2.5 THz	[17]
250 GHz	[9]
201 GHz	[3]

Switching Speeds

Consider the circuit in figure 3.3a, when the input voltage is zero the corresponding load line is given in figure 3.3b as line 1. The circuit is operating in the stable operating point A. When the

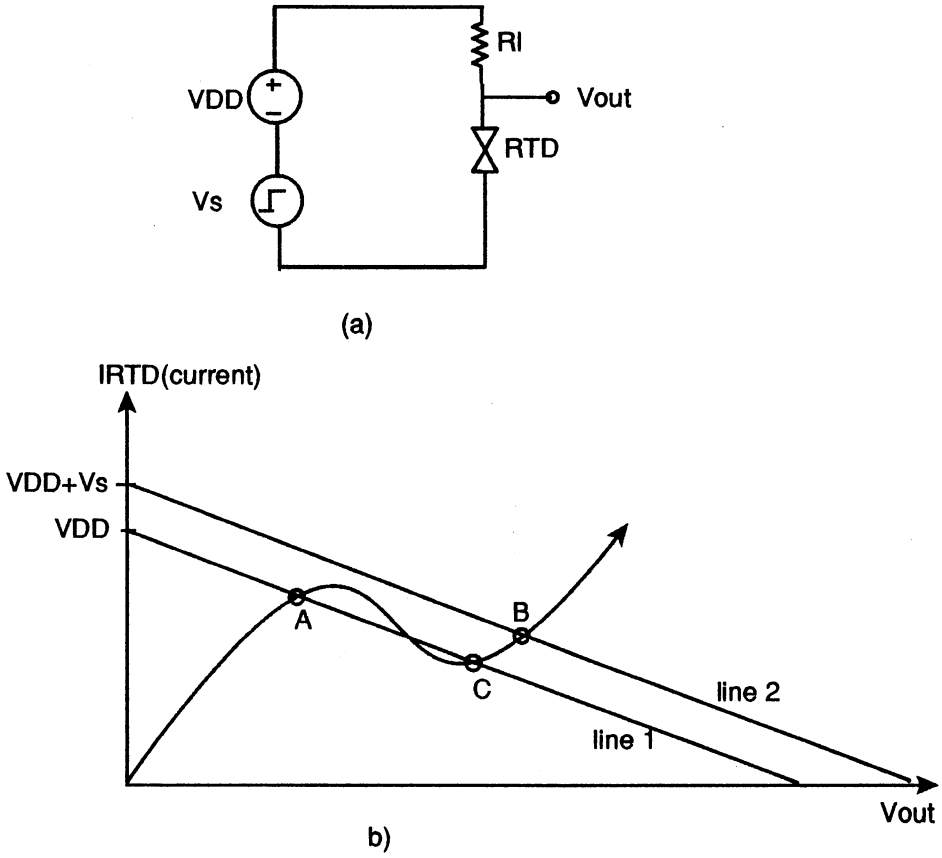

Figure 3.3 a) Resonant tunneling diode switching circuit. b) Current-voltage diagram of resonant tunneling diode with load lines.

input voltage is I_s the load line then corresponds to line 2 in figure 3.3b. The circuit then switches to the stable operating point B. The

switching time is given by[8],[13]

$$t_s = C_Q(V_c - V_{peak})/(I_p - I_v) \qquad (3.2)$$

where C_Q is the double barrier capacitance as in Figure 3.2, V_{peak} is the voltage corresponding to the resonant tunneling peak current I_p in the negative differential resistance region, and I_v is the valley current in the vegative differential resistance region. A switching time of 1.9 pS was experimentally recorded with such a switching circuit.[20] If the input voltage becomes zero again the circuit will be stable at the bias point C seen on line 1.

Resonant Tunneling Transistor Devices

Conventional Transistors

There have been several resonant tunneling transistors that are nothing more than a resonant tunneling diode in series with a field effect transistor.[1],[21],[22] One such device and its I-V characteristics can be seen in figures 3.4 and 3.5. The field effect transistor has the effect of being able to shift the negative differential resistance region, but it seriously hampers the speed performance of the device. The speed of the device is determined by the ability to modulate the channel of the field effect transistor. The field effect transistor also nullifies the area advantage of a pure resonant tunneling device.

Also of interest is the placement of a resonant tunneling diode

in the base of a bipolar junction transistor (figure 3.6).[5] The negative transconductance region can be seen in the I_c-I_b curves (figure 3.7) with V_{ce} held constant. Before this decrease in current gain the transistor behaves like a regular bipolar junction transistor.

Negative Resistance Stark Effect Transistor (NRSET)

If an atom is placed in an external electric field, its energy levels are altered: this phenomena is known as the Stark effect.[40a] This effect has been used to propose a resonant tunneling transistor in which the curent can be modulated by applying an electric field to the quantum well of a resonant tunneling structure to alter the energy levels in the quantum well.[2]

The schematic of this proposed device and its conduction band diagram can be seen in figure 3.8. The device consists of a resonant tunneling diode in series with another potential barrier which is contact with the base of the transistor. This barrier must be wide enough to prevent electron tunneling from the base to collector when a voltage is applied from base to emitter. The collector region must also be wide enough to prevent discrete energy levels from existing in the well formed by the collector region.

The characteristics of the I_c-V_{ce} curves are identical to a regualar resonant tunneling diode except that the negative differential resistance region can be shifted when a voltage is applied to the base of the transistor. This voltage applies an electric field to the quantum well in the resonant tunneling diode and

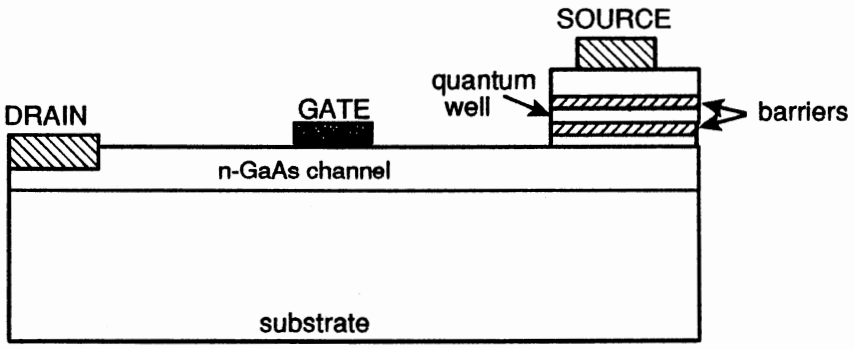

Figure 3.4 A MESFET with a resonant tunneling diode placed in its source.

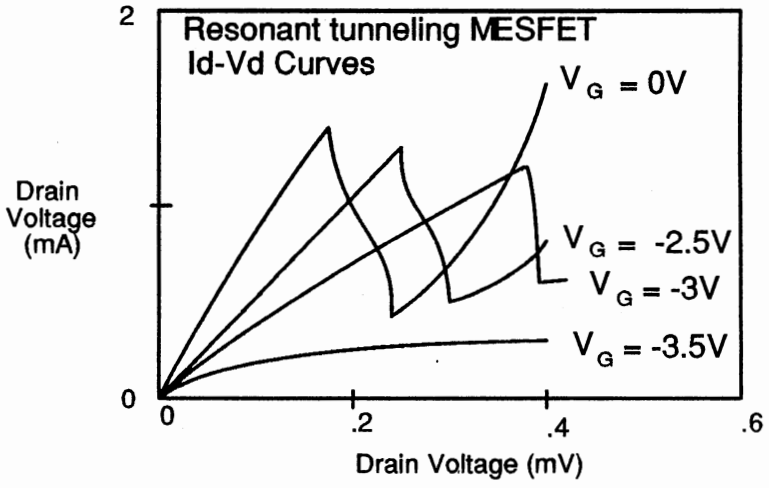

Figure 3.5 Id-Vd curves for a resonant tunneling MESFET

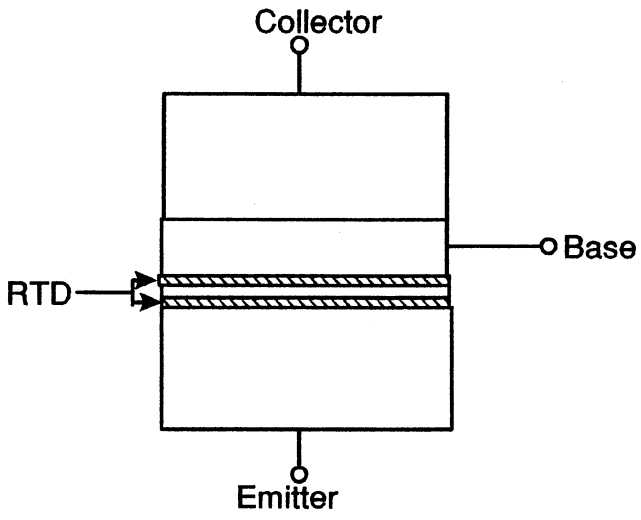

Figure 3.6 Bipolar junction transistor transistor with a resonant tunneling base

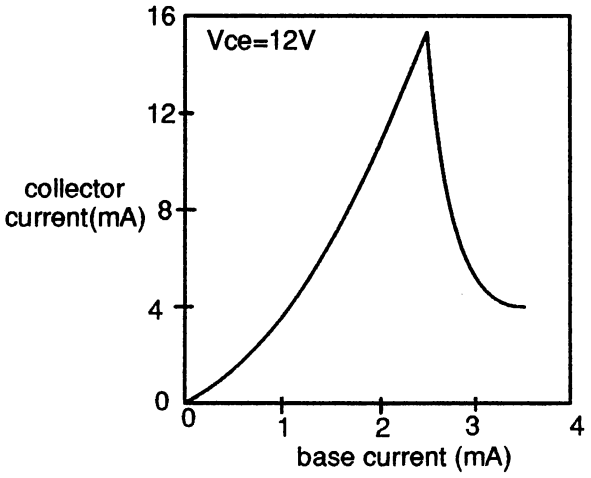

Figure 3.7 Ic-Ib curves for a bipolar junction transistor with a resonant tunneling base

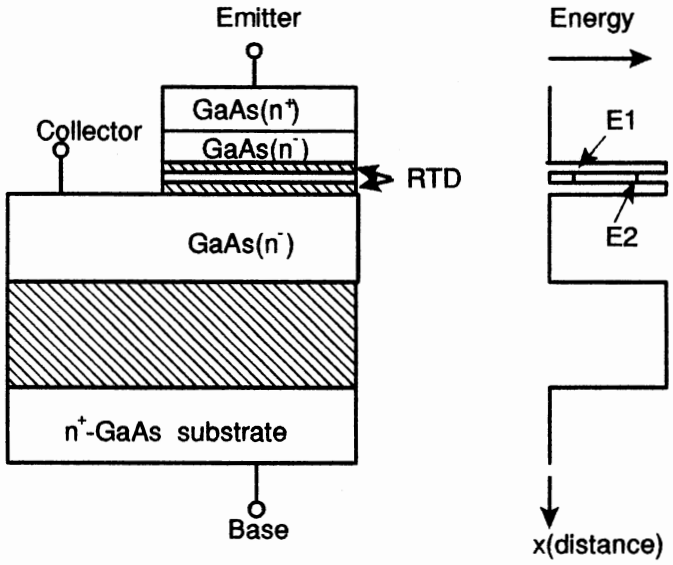

Figure 3.8 Cross-section schematic and energy diagram for the NRSET

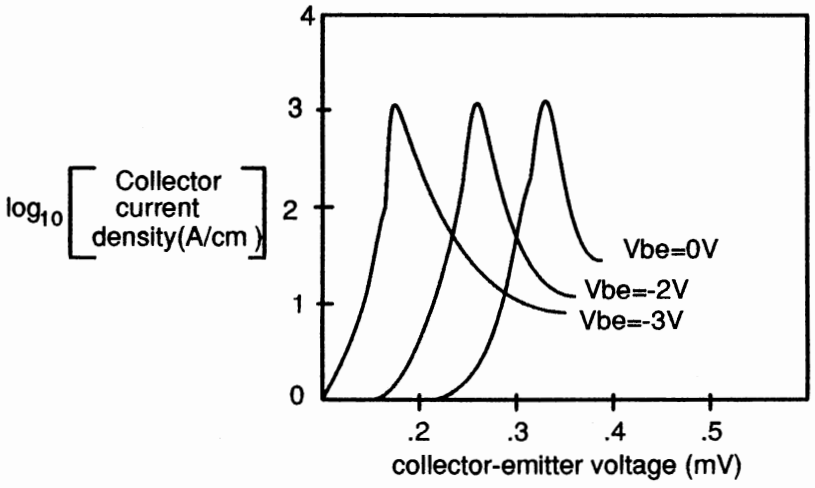

Figure 3.9 Log_{10}(collector current density)-V_{ce} transfer curves for NRSET

the energy levels in the quantum well are shifted via the Stark effect. This modulates the colector current in the device as seen in Figure 3.9.

Since tunneling is the main charge transport mechanism, this device features the high speed characteristics associated with tunneling structures. The draw back to the device is the large base voltage required to modulate I_C.

Bipolar Quantum Resonant Tunneling Transistor (BiQuaRTT)

A bipolar quantum resonant tunneling transistor (BiQuaRTT) is a transistor in which the tunneling current is directly controlled by modulating the potential inside the quantum well.[14] The BiQuaRTT consists of a resonant tunneling diode structure in which the quantum well is p-type doped and has a separate contact. The quantum well is equivalent to the base of a conventional bipolar transistor. The BiQuaRTT, unlike conventional resonant tunneling diodes, employs a wider band gap material in the emitter and collector region than in the base (quantum well) region. This prevents the device from having large leakage currents in the parasitic pn junctions at the base contact. The band structure diagram of this device can be seen in figure 3.10. A view of the structure of the BiQuaRTT can be seen in figure 3.13.

The I_C-V_{ce} common emmitter characteristics can be seen in figure 3.11. There are no negative differential resistance regions in the output characteristics because the base applied applied keeps the emitter lined up at the same energy level in the quantum well of the

device. There is however a negative transconductance region as the base voltage brings the emitter Fermi level just above the first energy level in the quantum well.

The small signal equivalent circuit can be seen in figure 3.12. C_{be} is the capacitor due to the sum of the depletion region capacitance and the barrier capacitance between the base and the emitter. C_{ce} is the double barrier capacitance, C_{sub} is the capacitance between the collector and substrate, and C_{bc} is the sum of the barrier capacitance between the base and collector and the capacitance due to the depletion region of the p-n junction between the base and collector. The resistors r_b, r_c, and r_e are the contact resistances at the base, collector, and emitter respectively. The resistance r_{be} is the resistance from the combined affecst of the reverse biased pn junction and the barrier between the base and the emitter.

This transistor has current voltage characteristics very similar to a conventional transistor and has all of the speed advantages of a device which operates on the tunneling principle. Although there is a p-n junction between the base and emitter of the BiQuaRTT just as there is in a conventional bipolar junction transistor; the p-n junction is never forward biased. This eliminates the problem of charging and discharging the large diffusion capacitor inhereent in conventional bipolar junction transistors. Typical current gains of 50 have been observed from this device.[14] This device has no actual size advantage over a conventional bipolar junction transistor, because the distance between the base and collector contacts is going

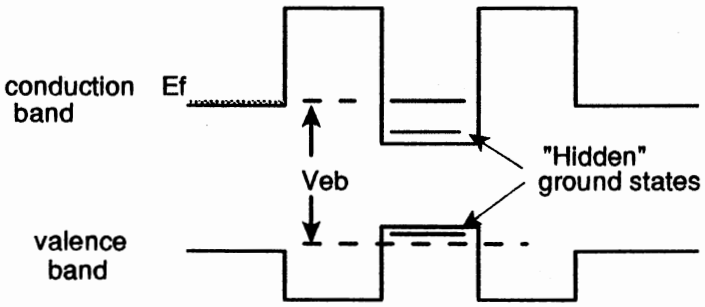

Figure 3.10 Energy diagram for the BiQuaRTT with Vce=0.

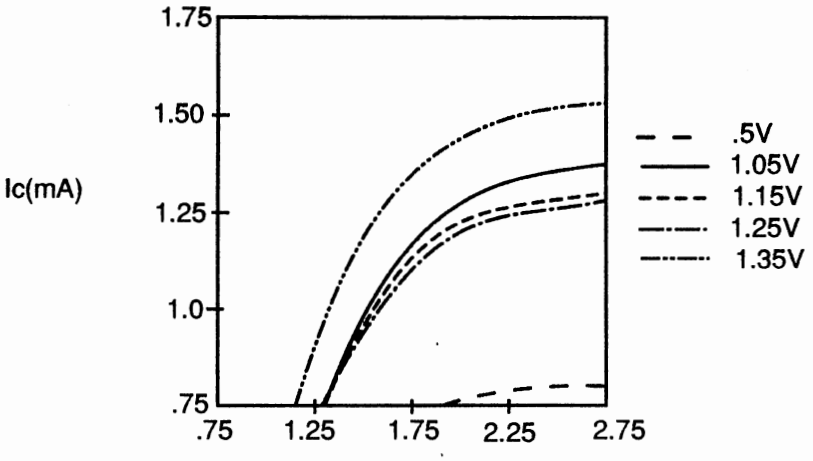

Figure 3.11 Transfer characteristics for a BiQuaRTT

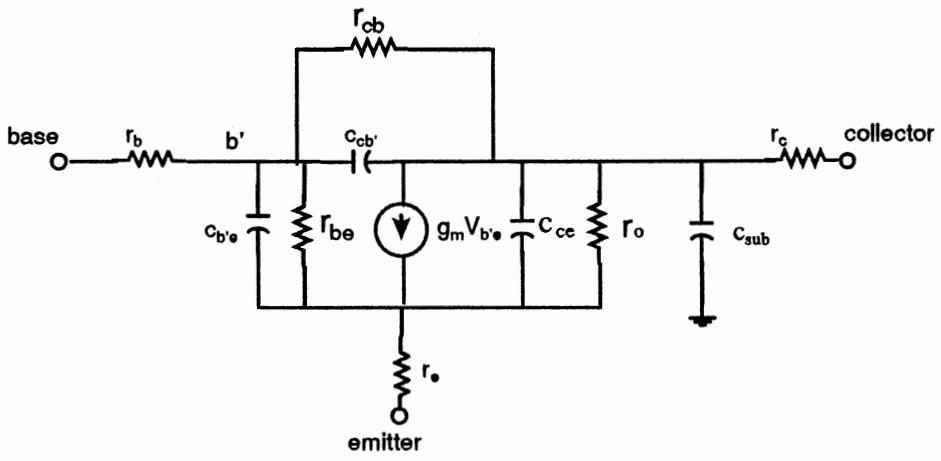

Figure 3.12 Equivalent circuit for a BiQuaRTT

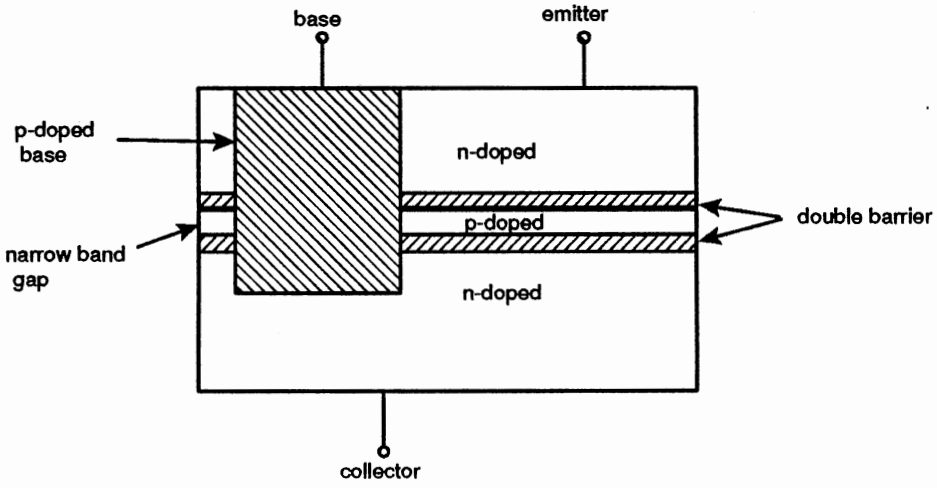

Figure 3.13 BiQuaRTT transistor

to be determined by the breakdown voltage between the base and collector just as in a conventional transistor.

Summary

To utilize the size and speed advantages of a quantum effect device, it is necessary to construct a device that has limitations based only on quantum effects. If the device size is limited by a load resistor or a conventional transistor, or the speed of operation is limited by a conventional transistor then the advantages inherent to the quantum effect device is not utilized. Among the devices discussed in this chapter only the NRSET and the BiQuaRTT utilizes the speed and/or size advantages of a quantum effect device of which the quantum effect is resonant tunneling.

CHAPTER IV

SIMULATION OF A RESONANT TUNNELING DIODE MEMORY CELL USING SPICE

SPICE Model for a Resonant Tunnelng Diode

A SPICE (Simulated Program with Integrated Circuit Emphasis) model which would reliably simulate a resonant tunneling diode was created. The SPICE model incorporated the circuit in figure 4.1. This circuit is the same as in figure 3.2 except the variable resistance R_T is replaced by coherent and incoherent tunneling components. The coherent tunneling component consists of the current source I_C, and the incoherent tunneling component consists of the "leak" resistor R_I.

I_C was obtained by solving for the transmission coefficient using the transfer matrix technique described in chapter II and solving the current density equation (equation 2.34). I_C was constructed on SPICE by summing the currents through three conventional diodes (figure 4.2). The first diode, D1, was used to achieve the characteristics when $V_{RTD} < V_p$. The second diode, D2, was used to achieve the current in the neqative differential resistance region: this was accomplished by decreasing V_2 as V_{RTD} increased. The third diode, D3, was used to achieve the current when V_{RTD} approached the potential of the barriers. The logarithmic slope of the coherent tunneling current

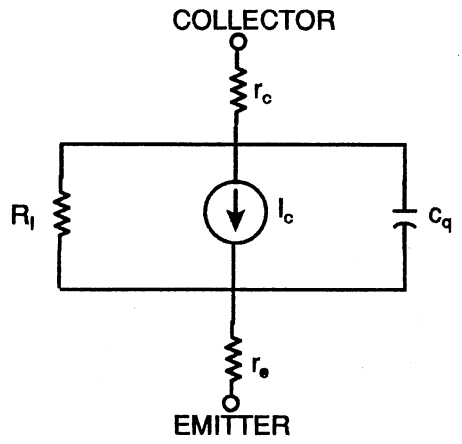

Figure 4.1 Circuit used for SPICE model of a resonant tunneling diode

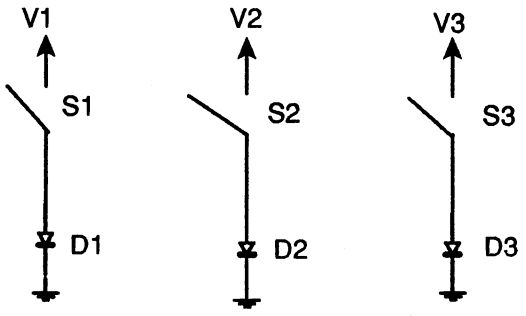

Figure 4.2 Circuit used for the simulation of coherent tunneling in the SPICE model of a resonant tunneling diode

curves was obtained by changing the emission coeficient in the diode SPICE .MODEL card. If there were more than one resonant energy level the quantum well then the same technique could be used to simulate the coherent tunneling current with additional conventional diodes. There should be 2N + 1 diodes, where N is the number of resonant energy levels in the quantum well. The switches; S1, S2, and S3 were used to turn the diodes on or off at the proper voltages. V1, V2, and V3 are functions of V_{RTD}.

An estimate for R_I was made from the peak to valley ratios reported by other authors. A peak to valley ratio of approximately two was selected from a review of the literature.

C_q was based on a worst case calculation. Assuming there are no depletion regions ouside of the barriers then

$$C_q = \frac{\varepsilon A}{L1 + L2 + W} \tag{4.1}$$

where ε is the weighted dielectric constant using the barrier and well materials, A is the active area of the device and L1, L2, and W are the lengths of the left barrier, right barrier, and quantum well respectively.

Simulated RTD

The resonant tunneling diode simulated consisted of a 1000Å n-doped $1X10^{18}/cm^{-3}$ GaAs emitter, a 40Å undoped AlGaAs barrier, an 40Å undoped GaAs quantum well, a 40Å undoped AlGaAs barrier, and a 1000 Å n-doped $1X10^{17}/cm^{-3}$ GaAs collector. The device has a cross-sectional

active area of .1μmX.1μm.

The calculation of the coherent current density is shown in Appendix A. R_c was calculated to be 2kΩ and R_e was calculated to be 200Ω, therefore R_e was ignored in the simulation. C_q was calculated to be .1fF and R_I was 600kΩ. A cross-section of this device and the current-voltage characteristics can be viewed in figure 4.3. The SPICE model of this resonant tunneling diode is shown in Appendix B.

It was assumed that the resonant tunneling diode could be manufactured with dimensions within 10% of the desired dimensions. Thus two other resonant tunneling diodes were simulated as worst case current-voltage conditions. The physical dimensions as well as the current-voltage characteristics of these devices can be seen in figure 4.4. It can be seen that a 10% increase in the first barrier and a 10% decrease in the second barrier causes the resonant voltage to shift from .24 volts to .20 volts and a 10% decrease in the first barrier and a 10% increase in the second barrier causes the resonant voltage to increase from .24 volts to .3 volts and the peak current increases from 1 milliampere to 1.5 milliampere. These changes are quite significant and should create the demand for great contol over the process when fabricating resonant tunneling devices.

RTD Memory Cell

A future application of a resonant tunneling device is as a very dense memory device. Memory structures have been proposed using a resonant tunnelig devices.[6][18] These devices consist of a resonant tunneling diode in series with a load resistor. This load resistor is

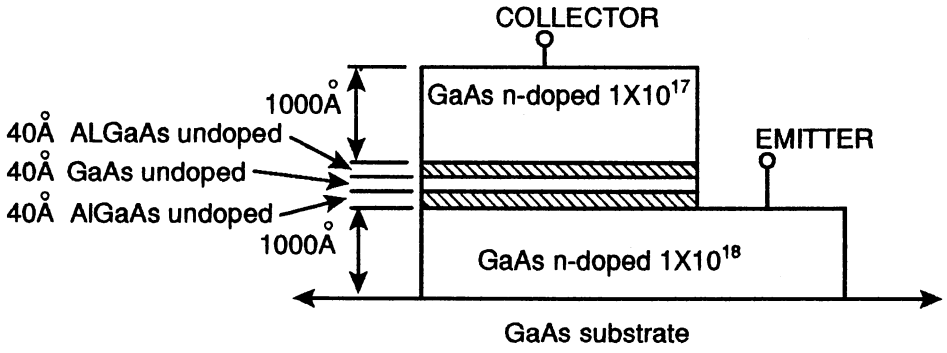

(a)

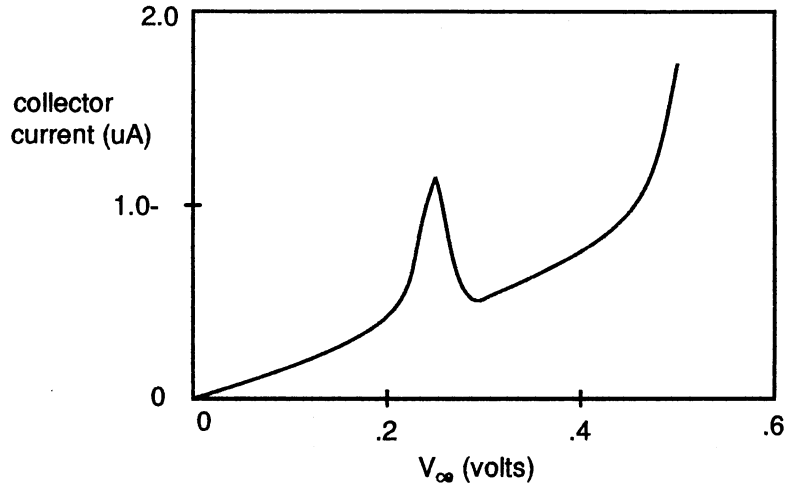

Figure 4.3 (a) cross-section for the resonant tunneling diode simulated with SPICE
(b) current-voltage relationship for the resonant tunneling diode simulated with SPICE

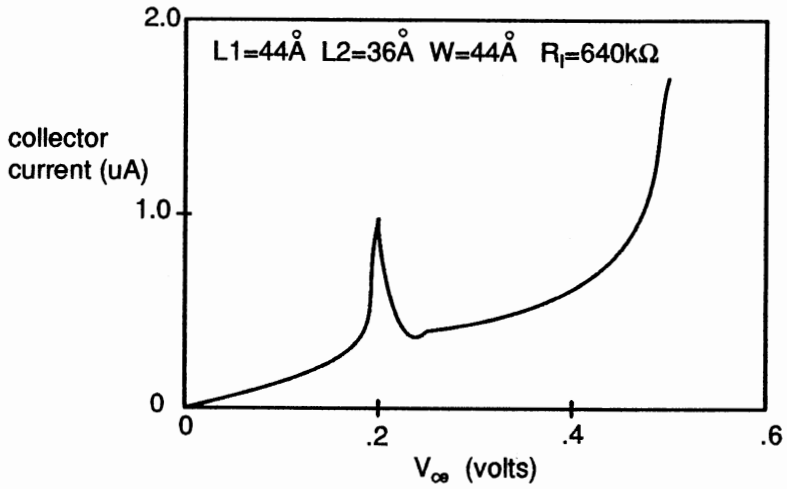

(a)

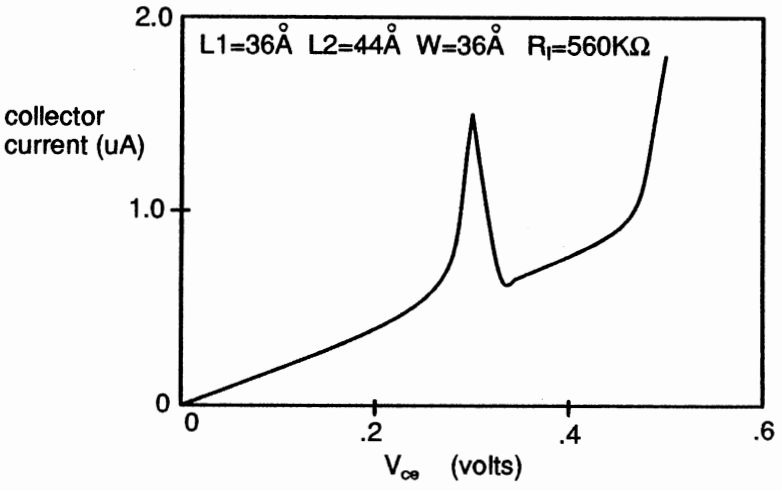

Figure 4.4 (a) and (b) worst case resonant tunneling diodes simulated with SPICE

not desirable for a very dense memory structure. This is mainly due to the low standby current required in a very dense memory structure.

This author would like to propose a memory cell that consists of a resonant tunneling diode in series with another resonant tunneling diode (figure 4.5). This memory cell has the

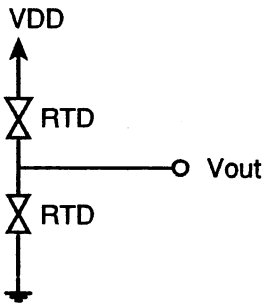

Figure 4.5 Schematic for a resonant tunneling diode memory cell.

advantage of having only circuit elements that are quantum mechanical charge transport devices, thus enabling small device sizes.

The operating points of this memory cell with a power suppty voltage of .65 volts can be seen by using the I-V characteristics of the top resonant tunneling device as a load curve on the I-V characteristics of the bottom device. Using the characteristic curves

of figure 4.3 the load curve of the memory cell can be viewed in figure 4.6. The operating points A and B are the ones desired to use for a logic low and a logic high respectively. There may be intermediate stable states, but these will be bypassed in the write operation.

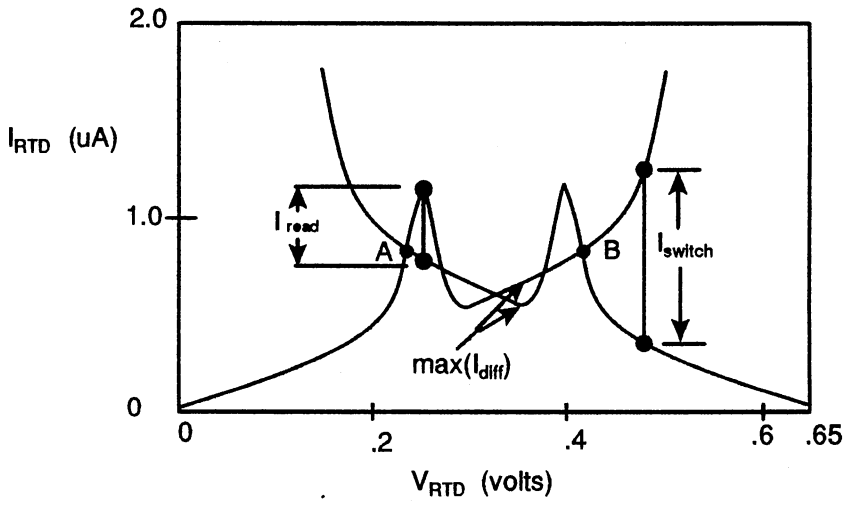

Figure 4.6 Load curves for a resonant tunneling memory cell

Writing to the memory cell is performed by either sourcing or sinking a current pulse to the output node of the memory cell. Sourcing current will cause the cell to store a logic one and sinking current will cause the cell to store a logic zero. Suppose a memory cell currently has a logic zero stored and is operating at the stable point A in figure 4.6. If a write of a logic one is then implemented

via a current pulse, when the current pulse is equal to I_{switch} each resonant tunneling diode will operate at the points that are connected by a verticle line of magnitude I_{switch} that is drawn on the load line curve as seen in figure 4.6. When the write current again has a magnitude of zero the memory cell will settle into the steady state B. The same argument applies for a write of a logic zero except the write current is negative with respect to the writing of a logic one.

Reading from the memory cell poses the largest problem. If too much current is drawn from the device then this causes a logic high to change to a logic low. There are two solutions to this problem. One is to use read/write circuitry where a read is followed by a write which restores the memory. The other solution is to limit the current when performing a read by scaling the channel width-length ratio of the pass transistor. The maximum current that can be sourced to or sunk from the memory device without disturbing the data in the cell can be seen in figure 4.6 and is labeled I_{read}. It is desired for I_{read} to be as large as possible, because it is necessary to charge up the bitline capacitance in the momorey device as quickly as possible. This will be the major restriction on the access time of the memory.

Simulation of RTD Memory Cell

The memory device shown in figure 4.7 was simulated using the SPICE models constructed. Writing to the memory cell which is composed using resonant tunneling diodes with the switching charateristics of figure 4.3 can be seen in figure 4.8. The worst case resonant tunneling diodes were used to find: minumum and maximum

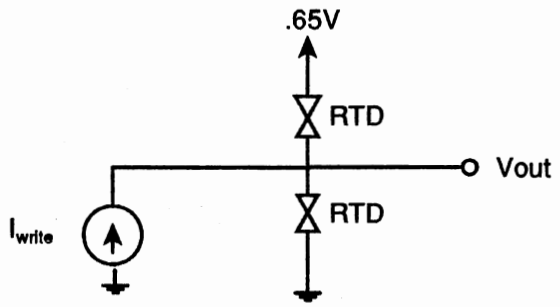

Figure 4.7 Circuit for simulation of writing to a resonant tunneling diode memory cell

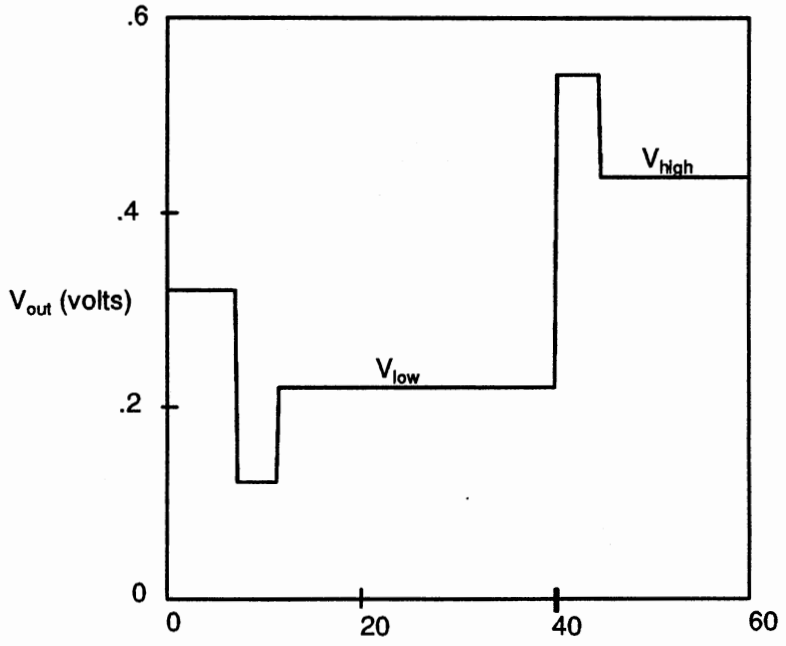

Figure 4.8 A trransient output of a write of a logic low and a logic high to to a resonant tunneling memory cell using a 1μA write current

TABLE III

SPECIFICATIONS FOR RTD MEMORY CELL

V_{high}	.38-.46 volt
V_{low}	.18-.27 volt
I_{write}	1.0 μAmp
I_{read}	0.3 μAmp
I_{bias}	1.0 μAmp

logic levels, maximum bias currents, maximum write currents, and read currents allowable. These numbers can be seen in table III.

This memory cell would have density compable to today's DRAM (Dynamic Random Access Memory) cell, but the proposed memory cell has the advantage of being static. The data stored remains stored as long as the device remains powered up. Another distinct advantage is that a DRAM only supplies charge to the bitline from the charge stored on the storage capacitor so sensing of the data is slow. The proposed RTD memory cell supplies charge from the voltage source through the RTD's, thus it has the potential of creating a larger voltage on the bitline more rapidly therefore speeding up the sensing time.

The major drawback to the proposed memory cell is standby power dissapation. It would be impossible to construct a memory chip with this type of storage cell and still have low enough power dissapation to achieve the densities desired. This problem would be solved if a RTD could be constructed that would have the theoretically possible exponentially large peak to valley current ratios. Then it would be

possible to bias the memory cell so that it would have only an extremely small current when the memory cell was operating in a stable logic state.

Conclusion

Many obstacles must be overcome to realize such a dense memory device. With today's technology the memory density would be metal line limited. The ability to lay metal lines with a width of .1μm and the ability to create a resonant tunneling device with such a small cross-sectional area. The object of this thesis is not to find ways to solve these problems, but to glimpse into the future and propose an alternative to the current memory structure which are reaching their physical limit in density. This limit is due to the breakdown of classical physics when dealing with such small dimensions thus the classical transistor ceases to operate in the manner for which it was designed. A resonant tunneling device does not have this problem because its characteristics are based on quantum mechanical effects.

CHAPTER V

CONCLUSIONS AND SUGGESTIONS FOR FURTHER RESEARCH

Resonant tunnelng theory, resonant tunneling devices, a SPICE model for a resonant tunneling diode, and a new resonant tunneling diode memory structure has been presented in this thesis. It has been noted that the scaling of a resonant tunneling device is not limited by classical mechanics as are conventinal devices. The replacement of conventional transistors will be a device in which its operation is based on quantum mechanical effects. The memory device presented in this thesis is not applicable with today's technology, but in the future possibly the processing techniques will become sharpened enough to fabricate such a device. There is much research to be done to improve the peak to valley current ratios of a resonant tunneling device which would make the memory cell proposed a feasible solution in the quest for very dense memories.

The most promising resonant tunneling device is the BiQuaRTT presented in chapter III. There is much research to be done in improving this device, creating a SPICE model for it, and applying it in useful circuitry.

BIBLIOGRAPHY

1. A. R. Bonnefoi, T. C. McGill, and R. D. Burnham, "Resonant tunneling transistors with controllable negative differential resistances", IEEE Elect. Dev. Lett. **EDL-6**(12) 626, 1985

2. A. R. Bonnefoi, D. H. Chow, and T. C. McGill, "Inverted base-collector tunnel transistors", Appl. Phys. Lett. **47**(8) 888, 1985

3. E. R. Brown, W. D. Goodhue, and T. C. L. G. Sollner, "Fundamental oscillations up to 200GHz in resonant tunneling diodes and new estimates of their maximum oscillation frequency from stationary-state tunneling theory", J. Appl. Phys., **64**(3) 1519, 1988

4. F. Capasso, K. Mohammed, and A. Y. Cho, "Resonant tunneling through double barriers, perpendicular quantum transport phenomena in superlattices and their device applications", IEEE Jour. of Quan. Elect. **QE-22**(9) 1853, 1986

5. F. Capasso, S. Sen, A. C. Gossard, A. L. Hutchinson, and J. H. English, "Quantum-well resonant tunneling bipolar transistor operating at room temperature", IEEE Elect. Dev. Lett. **EDL-7**(10) 573, 1986

6. F. Capasso, S. Sen, A. Y. Cho, and D. Sivco, "Resonant tunneling devices with multiple negative differential resistance and demonstration of a three-state memory cell for multiple-valued logic applications", IEEE Elect. Dev. Lett. **EDL-8**(7) 297, 1987

7. L. L. Chang, L. Esaki, and R. Tsu, "Resonant tunneling in Semiconductor double barriers", Appl. Phys. Lett. **24**(12) 593, 1974

8. D. D. Coon and H. C. Liu, "frequency limit of double barrier resonant tunneling oscillators", Appl. Phys. Lett. **49**(2) 94 1986

9. S. K. Diamond, E. Ozbay, M. J. W. Rodwell, D. M. Bloom, Y. C. Paw, E. Wolak, and J. S. Harris, "Fabrication of 200-GHz f_{max} resonant-tunneling diodes for integrated circuit and microwave applications", IEEE Elect. Dev. Lett. **10**(3) 104, 1989

10. L. Esaki and R. Tsu, "Superlattice and negative differential conductivity in semiconductors", IBM Jour. of Res. Dev. **14** 61, 1970

11. M. E. Hines, "Principles for Esaki diode applications", Bell Syst. Tech. J. **39** 477, 1960

12. L. D. Landau and E. M. Lifshitz, Quantum Mechanics 2nd ed., Pergamon Press, 1965

13. H. C. Liu and D. D. Coon, "heterojunction double barrier diodes for logic applications", Appl. Phys. Lett. **50**(18) 1246, 1987

14. M. A. Reed, W. R. Frensley, R. J. Matyi, J. N. Randall, and A. C. Seabaugh, Realization of a three-terminal resonant tunneling device: The bipolar quantum resonant tunneling transistor", Appl. Phys. Lett. **54**(11) 1034, 1989

15. B. Ricco and M. Y. Azbel, "physics of resonant tunneling. The one-dimensional double-barrier case", Phys. Rev. B **29**(4) 1970, 1984

16. J. Soderstrom and T. G. Anderson, "A multiple-state memory cell based on the resonant tunneling diode", IEEE Elect. Dev. Lett. **9**(5) 200, 1988

17. T. C. L. G. Sollner, W. D. Goodhue, P. E. Tannenwald, C. D. Parker, and D. D. Peck, "Resonant tunneling through quantum wells at frequencies up to 2.5 THz", Appl. Phys. Lett. **43**(6) 588, 1983

18. A. D. Stone and P. A. Lee, "Effect of inelastic processes on resonant tunneling in one dimension", Phys. Rev. Lett. **54**(11), 1985

19. R. Tsu and L. Esaki, "Tunneling in a finite superlattice", Appl. Phys. Lett. **22**(11) 562, 1973

20. J. F. Whitaker, G. A. Mourou, T. C. L. G. Sollner, and W. D. Goodhue, "Picosecond switching time measurement of a resonant tunneling diode", Appl. Phys. Lett. **53**(5) 385, 1988

21. T. K. Woodward, T. C. McGill, and R. D. Burnham, "Experimental realization of a resonant tunneling transistor", Appl. Phys. Lett. **50**(8) 451, 1987

22. T. K. Woodward, T. E. McGill, H. F. Chung, and R. D. Burnham, "integration of a resonsant-tunneling structure with a metal-semiconductor field-effect transistor", Appl. Phys. Lett. **51**(19) 1542, 1987

APPENDIX A

SOLUTION OF SCHROEDINGERS WAVE EQUATION

FOR DOUBLE POTENTIAL BARRIERS

INTRODUCTION:

This report discusses the procedure for solving the time independent form of Schroedingers Wave Equation (SWE) for two potential barriers separated by a single quantum well. The transmission coefficient is obtained for particles that have energies less than the potential of the barriers. Locations of resonant tunneling energies are obtained.

SOLVING SWE FOR DOUBLE POTENTIAL BARRIER:

Starting with SWE

$$-\frac{h^2}{2m}\frac{\partial^2\Psi}{\partial x^2} + V(y)\Psi = jh\frac{\partial\Psi}{\partial t} \tag{1}$$

Let Ψ_{inc} be a wave propagating in the positive x direction in region I.

$$\Psi_{inc} = Ae^{j(kx-\omega t)} \tag{2}$$

Let the reflected wave at the barrier in region I be

$$\Psi_{ref} = Be^{j(-kx-\omega t)} \tag{3}$$

To show that (2) and (3) are solutions to (1) in region I where v(y)=0:

$$-\frac{h2}{2m}\frac{\partial 2\Psi}{\partial x^2} = jh\frac{\partial \Psi}{\partial t} \tag{4}$$

$$\frac{\partial \Psi_{inc}}{\partial t} = -j\omega\Psi_{inc} \tag{5}$$

$$\frac{\partial \Psi_{inc}}{\partial x} = jk\Psi_{inc} \tag{6}$$

$$\frac{\partial^2 \Psi_{inc}}{\partial x^2} = -k^2\Psi_{inc} \tag{7}$$

Subst (5),(7) into (4)

$$\frac{h^2}{2m}k^2 = h\omega \tag{8}$$

$$E=h\omega \tag{9}$$

$$k = \frac{(2mE)^{1/2}}{h} \tag{10}$$

From superposition

$$\Psi_1 = \Psi_{inc} + \Psi_{ref} = (Ae^{jkx} + Be^{-jkx})e^{-j\omega t} \tag{11}$$

In reqion II we have

$$\Psi^+ = Ce^{j(kx-\omega t)} \tag{12}$$

$$k = j\frac{(2m(V_0-E))^{1/2}}{h} \tag{13}$$

$$k = j\alpha \tag{14}$$

$$\alpha = \frac{(2m(V_0-E))^{1/2}}{h} \tag{15}$$

$$\Psi_2^+ = Ce^{-\alpha x}e^{-\omega t} \tag{16}$$

Substituting (15) and (16) into (1) and setting $V(y)=V_0$ we obtain the equation $E=h\omega$; therefore showing 16 also satisfies SWE. We can again use superposition obtaining

$$\Psi_2 = (Ce^{-\alpha x} + De^{\alpha x})e^{-\omega t} \tag{17}$$

Solutions to SWE can now be written for each region giving the following:

Region I

$$\Psi_1 = (Ae^{jkx} + Be^{-jkx})e^{-j\omega t} \tag{18}$$

Region II:

$$\Psi_2 = (Ce^{-\alpha x} + De^{\alpha x})e^{-j\omega t} \tag{19}$$

Region III:

$$\Psi_3 = (Fe^{jkx} + Ge^{-jkx})e^{-j\omega t} \tag{20}$$

Region IV:

$$\Psi_4 = (He^{-\alpha x} + Ie^{\alpha x})e^{-j\omega t} \tag{21}$$

Region V:

$$\Psi_5 = Ne^{jkx}e^{-j\omega t} \tag{22}$$

In Region V there is no wave traveling in the negative x direction, because there is no barrier to reflect it.

To solve for the constants we equate the wave functions and their derivatives at each discontinuity.

$$\Psi_N(x) = \Psi_{N+1}(x) \tag{23}$$

$$\left.\frac{\Psi_N}{x}\right|_x = \left.\frac{\Psi_{N+1}}{x}\right|_x \tag{24}$$

The constants can be written in matrix form as follows:

$$A = \frac{1}{2}\begin{bmatrix} 1 - \frac{\alpha}{jk} & 1 + \frac{\alpha}{jk} \end{bmatrix}\begin{bmatrix} C \\ D \end{bmatrix} \tag{25}$$

$$B = \frac{1}{2}\begin{bmatrix} 1 + \frac{\alpha}{jk} & 1 - \frac{\alpha}{jk} \end{bmatrix}\begin{bmatrix} C \\ D \end{bmatrix} \tag{26}$$

$$C = \frac{1}{2}\begin{bmatrix} (1 - j\frac{k}{\alpha})e^{(jk - \alpha)L} & (1 + \frac{jk}{\alpha})e^{(-jk + \alpha)L} \end{bmatrix}\begin{bmatrix} F \\ G \end{bmatrix} \tag{27}$$

$$D = \frac{1}{2}\begin{bmatrix} (1 + j\frac{k}{\alpha})e^{(jk-\alpha)L} & (1 - j\frac{k}{\alpha})e^{(-jk-\alpha)L} \end{bmatrix}\begin{bmatrix} F \\ G \end{bmatrix} \tag{28}$$

$$F = \frac{1}{2}\begin{bmatrix} (1 - \frac{\alpha}{jk})e^{(-jk-\alpha)(L+W)} & (1 + \frac{\alpha}{jk})e^{(-jk+\alpha)(L+W)} \end{bmatrix}\begin{bmatrix} H \\ I \end{bmatrix} \tag{29}$$

$$G = \frac{1}{2}\begin{bmatrix} (1 + \frac{\alpha}{jk})e^{(jk-\alpha)(L+W)} & (1 - \frac{\alpha}{jk})e^{(jk+\alpha)(L+W)} \end{bmatrix}\begin{bmatrix} H \\ I \end{bmatrix} \tag{30}$$

$$H = \frac{1}{2}\begin{bmatrix} (1 - j\frac{k}{\alpha})e^{(jk-\alpha)(2L+W)} \end{bmatrix}\begin{bmatrix} N \end{bmatrix} \tag{31}$$

$$I = \frac{1}{2}\begin{bmatrix} (1 + j\frac{k}{\alpha})e^{(jk-\alpha)(2L+W)} \end{bmatrix}\begin{bmatrix} N \end{bmatrix} \tag{32}$$

To find the transmission corfficient of the double barrier, it is necessary to find I_{out}/I_{in}. (where I_{out} = intensity of the wave

traveling in the positive x direction in region V and I_{in} = intensity of the positive traveling wave in Region I.

$$I_{out} = \Psi^*_{out}\Psi_{out}(\frac{hk}{m}) = N^*N(\frac{hk}{m}) \tag{33}$$

$$I_{in} = A^*A\frac{hk}{m} \tag{34}$$

$$T = \frac{I_{out}}{I_{in}} = \frac{N^*N}{A^*A} \tag{35}$$

Working backwards from equations (32) - (25), A can be found in terms of N and the coefficient N will cancel in equation (35). I therefore set the coefficient N to 1 and solved the matrices for A using MATRIXX.

APPENDIX B

SPICE MODEL FOR A RESONANT TUNNELING DIODE

```
E3 7 0 POLY(1) 2 0 -.45 1
V1 3 10 0
V2 5 11 0
V3 7 12 0
V4 2 18 0
V5 1 20 0
D1 4 0 DMOD1
D2 6 0 DMOD2
D3 8 0 DMOD3
F1 18 0 V1 1
F2 18 0 V2 1
F3 18 0 V3 1
S1 10 4 2 0 SMOD1
S2 11 6 2 0 SMOD2
S3 12 8 2 0 SMOD3
RS 20 2 1
RI 2 0 900
C1 2 0 778F
.MODEL DMOD1 D (IS=50E-06 N=3)
.MODEL DMOD2 D (IS=50E-06 N=3)
.MODEL DMOD3 D (IS=.3E-06 N=3.2)
.MODEL SMOD1 VSWITCH (RON=1 VON=.23 VOFF=.231)
.MODEL SMOD2 VSWITCH (RON=1 VON=.231 VOFF=.23)
.MODEL SMOD3 VSWITCH (RON=1 VON=.45 VOFF=.44)
.DC VRTD 0 .55 .01
.PLOT DC I(V4)
.PROBE
.END
```

APPENDIX C

MATHCAD FILE FOR CALCULATING

THE COHERENT TUNNELING CURRENT

OF A RESONANT TUNNELING DIODE

$h := 4.1357 \cdot 10^{-15}$ $\quad d1 := 40 \cdot 10^{-10}$ $\quad d2 := 40 \cdot 10^{-10}$ $\quad w := 40 \cdot 10^{-10}$

$hb := 6.528 \cdot 10^{-16}$ $\quad Vo := .5$ $\quad Ef := .04001$

$mass := 9.11 \cdot 10^{-31}$ $\quad C := 3 \cdot 10^{8}$ $\quad q := 1.6 \cdot 10^{-19}$

$m := .511 \cdot 10^{6} \cdot C^{-2}$ $\quad kb := 86.14 \cdot 10^{-6}$

$me := .07 \cdot m$

$Te := 100$

$\varepsilon b := 12.7$ $\quad \varepsilon w := 10$

$$Fb(V) := \frac{V}{d1 + d2 + w \cdot \frac{\varepsilon b}{\varepsilon w}} \qquad Fw(V) := \frac{\varepsilon b}{\varepsilon w} \cdot Fb(V)$$

$$\alpha 1(V, x, E) := \frac{1}{hb} \cdot \sqrt{2 \cdot me \cdot (Vo - E - Fb(V) \cdot x)}$$

$$\alpha 2(V, x, E) := \frac{1}{hb} \cdot \sqrt{2 \cdot me \cdot (Vo + w \cdot (Fb(V) - Fw(V)) - E - Fb(V) \cdot x)}$$

$$k(V, x, E) := \frac{1}{hb} \cdot \sqrt{2 \cdot me \cdot (E - (Fw(V) - Fb(V)) \cdot d1 + Fw(V) \cdot x)}$$

$$c1 := \frac{\sqrt{2 \cdot me}}{hb} \qquad c2(V) := \frac{2}{3 \cdot Fb(V)}$$

$$\alpha 11(V,E) := c1 \cdot c2(V) \cdot \left[-\sqrt{(Vo - E - Fb(V) \cdot d1)^3} + \sqrt{(Vo - E)^3} \right]$$

$$c3(V,E) := \sqrt{(Vo - Fw(V) \cdot w - E - Fb(V) \cdot d1)^3}$$

$$\alpha 22(V,E) := c1 \cdot c2(V) \cdot \left[-\sqrt{(Vo - Fw(V) \cdot w - E - Fb(V) \cdot (d1 + d2))^3} + c3(V,E) \right]$$

$$k1(V,E) := c1 \cdot \frac{2}{3 \cdot Fw(V)} \cdot \left[\sqrt{(E + Fb(V) \cdot d1 + Fw(V) \cdot w)^3} - \sqrt{(E + Fb(V) \cdot d1)^3} \right]$$

$$k0(E) := \frac{1}{hb} \cdot \sqrt{2 \cdot me \cdot E}$$

$$Mab(V,E) := \frac{1}{2} \cdot \begin{bmatrix} 1 - i \cdot \frac{\alpha 1(V,0,E)}{k0(E)} & 1 + i \cdot \frac{\alpha 1(V,0,E)}{k0(E)} \\ 1 + i \cdot \frac{\alpha 1(V,0,E)}{k0(E)} & 1 - i \cdot \frac{\alpha 1(V,0,E)}{k0(E)} \end{bmatrix}$$

$$B(V,E) := e^{\alpha 11(V,E)}$$

$$Mbc(V,E) := \begin{bmatrix} e^{-\alpha 11(V,E)} & 0 \\ 0 & B(V,E) \end{bmatrix}$$

$$C(V,E) := 1 + i \cdot \frac{k(V,d1,E)}{\alpha1(V,d1,E)} \qquad D(V,E) := 1 - i \cdot \frac{k(V,d1,E)}{\alpha1(V,d1,E)}$$

$$Mcd(V,E) := \frac{1}{2} \cdot \begin{bmatrix} C(V,E) & D(V,E) \\ D(V,E) & C(V,E) \end{bmatrix}$$

$$G(V,E) := e^{i \cdot k1(V,E)}$$

$$Mde(V,E) := \begin{bmatrix} e^{-(i \cdot k1(V,E))} & 0 \\ 0 & G(V,E) \end{bmatrix}$$

$$H(V,E) := 1 - i \cdot \frac{\alpha2(V,d1 + w,E)}{k(V,d1 + w,E)}$$

$$K(V,E) := 1 + i \cdot \frac{\alpha2(V,d1 + w,E)}{k(V,d1 + w,E)}$$

$$Mef(V,E) := \frac{1}{2} \cdot \begin{bmatrix} H(V,E) & K(V,E) \\ K(V,E) & H(V,E) \end{bmatrix}$$

$$L(V,E) := e^{\alpha22(V,E)}$$

$$Mfg(V,E) := \begin{bmatrix} -\alpha 22(V,E) & 0 \\ 0 & L(V,E) \end{bmatrix}$$

$$kf(V,E) := \frac{1}{hb}\cdot\sqrt{2\cdot me\cdot(E+V)}$$

$$N(V,E) := 1 + i\cdot\frac{kf(V,E)}{\alpha 2(V,(d1+w+d2),E)}$$

$$O(V,E) := 1 - i\cdot\frac{kf(V,E)}{\alpha 2(V,(d1+w+d2),E)}$$

$$Mgh(V,E) := \frac{1}{2}\cdot\begin{bmatrix} N(V,E) & O(V,E) \\ O(V,E) & N(V,E) \end{bmatrix}$$

$$Mtot(V,E) := Mab(V,E)\cdot Mbc(V,E)\cdot Mcd(V,E)\cdot Mde(V,E)\cdot Mef(V,E)\cdot Mfg(V,E)\cdot Mgh(V,E)$$

$$T(V,E) := \frac{1}{\left[\left|Mtot(V,E)_{1,1}\right|\right]^2}$$

$$j := 1..39$$

$$V_j := \frac{j}{100}$$

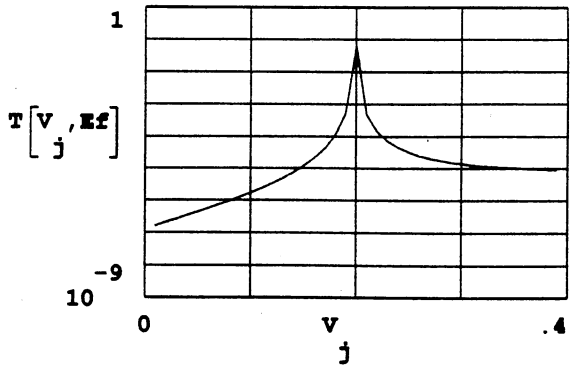

$$f(V,E) := \ln\left[\frac{1 + e^{\frac{Ef-E}{kb \cdot Te}}}{1 + e^{\frac{Ef-E-V}{kb \cdot Te}}}\right]$$

$E1 := .15$

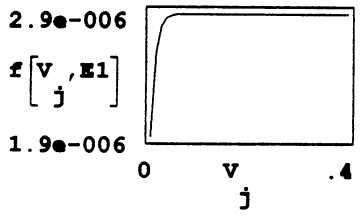

$$J(V) := \int_{.0001}^{.15} T(V,E) \cdot f(V,E)\, dE$$

$z := 1 \,..15$

$$V1_z := \frac{z}{30}$$

VITA

Darryl G. Walker

Candidate for the Degree of

Master of Science

Thesis: RESONANT TUNNELING BASED DEVICES WITH MEMORY APPLICATIONS

Major Field: Electrical Engineering

Biographical:

Personal Data: Born in Brownsville, Tennessee, October 28, 1964, the son of William B. and Birdie Walker.

Education: Graduated from Keyes Senior High School, Keyes, Oklahoma, in May 1982: received Bachelor of Science Degree in Electrical Engineering form Oklahoma State University in December, 1987; completed requirements for the Master of Science degree at Oklahoma State University in July, 1990.

Professional Experience: Teaching Assistant, Department of Electrical Engineering, Oklahoma state university, August, 1987 to December 1988; DRAM design engineer at Texas Instruments, Houston, Texas, August 1989 to present.